A Topological Study of the Transition States of the Hydrogen Exchange and Dehydrogenation Reactions of Methane on a Zeolite Cluster

N. B. Okulik

Departamento de Química, Facultad de Agroindustrias, UNNE. Cte. Fernández 755. (3700) Sáenz Peña, Chaco, Argentina

R. Pis Diez* and A. H. Jubert

CEQUINOR, Centro de Química Inorgánica (CONICET-UNLP), Departamento de Química, Facultad de Ciencias Exactas, UNLP, C.C. 962, 1900 La Plata, Argentina

P. M. Esteves† and C. J. A. Mota

Instituto de Quimica, Departmento Quimica Organica, Universidade Federal do Rio de Janeiro, Cidade Universitaria, CT Bloco A, 21949-900, Rio de Janeiro, Brazil

Received: December 31, 2000; In Final Form: May 10, 2001

The transition states of the hydrogen exchange and dehydrogenation reactions of methane on a zeolite acid site are studied within the framework of the density functional theory and the atoms-in-molecules theory. The transition state for the hydrogen exchange reaction is found to be characterized by a slightly ionic interaction between a distorted CH_5^+ structure and the negatively charged zeolite. No free carbocation is found. The dehydrogenation reaction presents a transition state in which three different fragments can be well identified, namely, an almost planar CH_3^+ structure, a H_2 pseudomolecule, and the negatively charged zeolite. The interaction between the fragments can be described as a closed-shell one, typical of rather ionic systems.

Introduction

Zeolites are among the most employed acid catalysts in hydrocarbon transformation processes mainly due to their high activity, reactivity, and thermal stability.[1,2] Such processes are of importance in the petrochemical industry as well as in the production of chemical compounds. When methane is allowed to interact with a zeolite acid site (ZOH), for example, it can lead whether to a hydrogen exchange reaction 1 or to a dehydrogenation process (eq 2)

$$ZOH^* + CH_4 \rightarrow ZOH + H^*CH_3 \quad (1)$$

The proposed reaction mechanisms for the above process

$$ZOH + CH_4 \rightarrow ZOCH_3 + H_2 \quad (2)$$

indicate the presence of carbocations.[3] A carbonium ion in which the carbon atom is coordinated to five hydrogen atoms is involved in the hydrogen exchange reaction 1, whereas a carbenium ion, a carbon atom coordinated to three hydrogen atoms, takes part in the dehydrogenation reaction 2.

The structural and acid site properties of zeolites can be determined experimentally with accuracy nowadays.[4] Their catalytic behavior, however, is mainly characterized by a complex combination of reactions on the active sites on the one side and the adsorption and diffusion of reactants in the microporous channel system on the other side. These last two phenomena, unfortunately, are quite difficult to study experimentally.[4] Thus, their investigation from a theoretical point of view becomes an appealing alternative to aid in our understanding of the catalytic behavior of zeolites.

Different theoretical methods are broadly used to study the mechanisms of zeolite-catalyzed reactions such as those mentioned above. Several authors using different methodologies agree that no free methonium ions are formed as intermediates in the hydrogen exchange reaction of methane on zeolite acid sites.[5−10] A transition state (TS) with a structure in which the carbon atom becomes pentacoordinated, as in a free methonium ion, is formed instead. The CH_5^+ cation is found to be bonded to the oxygen atoms in the zeolite through two hydrogen atoms. Their findings also suggest that the bonding in the TS is essentially covalent. It is interesting to note that van Santen indicates that the TS for reactions on zeolites other than those involving hydrogen exchange ones usually presents a quite ionic character.[9]

On the other hand, other theoretical studies indicate that the dehydrogenation reaction of methane on a zeolitic acid site seems to involve a different transition state in which a carbenium ion, CH_3^+, interacts with the basic site of the zeolitic system and molecular hydrogen evolves as a reaction product.[11,12] No discussion concerning the bonding nature in the TS for the dehydrogenation reaction is given in these works.

Finally, other authors make a detailed comparison of the TS for both reactions using the density functional theory (DFT) and the Hartree−Fock method.[13−15] These works agree that a carbonium ion is covalently bonded to the zeolite via two hydrogen atoms in the TS in reactions of type 1 whereas a carbenium ion is only weakly bonded to the oxygen atoms in

* Corresponding author.

† Present address: University of Southern California, Donald P & Katherine B Loker Hydrocarbon Research Institute, University Park, Los Angeles, CA 90089.

10.1021/jp0046142 CCC: $20.00
Published on Web 06/28/2001

the zeolite through the carbon atom in the TS in dehydrogenation reactions (eq 2).

It should be stressed that all those conclusions mentioned above concerning the nature of the bond between the carbocations and the zeolitic acid sites are achieved by considering only Mulliken charges and/or bond lengths and bond energies. Thus, as a further contribution to this very interesting subject, the hydrogen exchange and dehydrogenation reactions of methane on a zeolitic system are studied in this work within the density functional theory framework.[16] The corresponding transition states are obtained, and their structures are characterized using the topology of the electronic charge density within the atoms-in-molecules method[17,18] in order to shed light into the nature of the interaction of alkanes with zeolite acid sites.

Method and Calculation Details

The transition states for the hydrogen exchange and dehydrogenation reactions of methane on a zeolitic system are investigated within the framework of the density functional[16] and the atoms-in-molecules theories.[17,18]

The present study is carried out using Becke's three-parameter density functional[19] and the Lee, Yang, and Parr functional to describe gradient-corrected correlation effects,[20] leading to the well-known B3LYP method. The basis set used is 6-31G**. All the calculations are accomplished using the Gaussian 94 package.[21]

The zeolite acid site is represented by a linear T3 cluster (T = Si, Al) in which the mid tetrahedron contains the Al atom. The OH groups attached to the silicon atoms in the terminal tetrahedrons are replaced by hydrogen atoms to avoid dangling bonds associated with the finiteness of the cluster model.

The geometries of methane, dihydrogen, CH_5^+, CH_3^+, and the T3 cluster are optimized without constrains. These systems are confirmed as true minima by the presence of real harmonic frequencies after the corresponding vibrational analysis. The TS for the hydrogen exchange and dehydrogenation reactions of methane on the T3 system are optimized using the eigenvector following method,[22] and they are characterized as first-order saddle points by the presence of one and only one imaginary harmonic vibrational frequency. Both the geometry and transition state optimizations as well as the frequency calculations are performed at the above-mentioned level of theory.

The topological analysis and the evaluation of local properties are accomplished by means of the PROAIM program.[23] The densities used in the topological analysis are obtained through single point calculations on the above geometries and transition states using the B3LYP level of theory and the 6-311++G** basis set provided by the G94 package.

Atoms-in-Molecules Theory: An Overview. The theory of atoms in molecules (AIM)[17,18] provides a simple, rigorous, and elegant definition of atoms and bonds. This theory is based on the critical points (CP) of the molecular electronic charge density, $\rho(\mathbf{r})$. These are points where the electronic density gradient, $\nabla\rho(\mathbf{r})$, vanishes and are characterized by the three eigenvalues, λ_i ($i = 1, 2, 3$), of the Hessian matrix of $\rho(\mathbf{r})$. The CP's are labeled as (r, s) according to their rank, r (number of nonzero eigenvalues), and signature, s (excess of positive over negative eigenvalues).

Four types of CP's are of interest in molecules: (3, −3), (3, −1), (3, +1), and (3, +3). A (3, −3) point corresponds to a maximum in $\rho(\mathbf{r})$, characterized by $\nabla^2\rho(\mathbf{r}) < 0$ and occurs generally at the nuclear positions. A (3, +3) point indicates electronic charge depletion, and it is characterized by $\nabla^2\rho(\mathbf{r}) > 0$. It is also known as box critical point. (3, +1) points, or ring critical points, are saddle points. Finally, a (3, −1) point, or bond critical point, is generally found between two neighboring nuclei, indicating the existence of a bond between them.

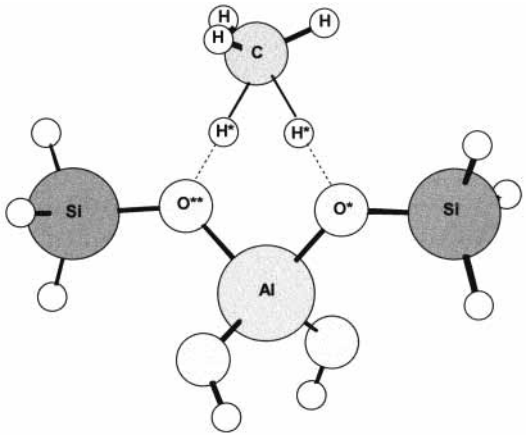

Figure 1. Transition state geometry for the hydrogen exchange reaction of methane on a T3 cluster. See Tables 1 and 2 for labels.

Several properties which can be evaluated at the bond CP constitute very powerful tools to classify a given structure and to analyze the interactions between two fragments.[24,25] The two negative eigenvalues of the Hessian matrix (λ_1 and λ_2) measure the degree of contraction of $\rho(\mathbf{r})$ perpendicular to the bond toward the critical point, while the positive eigenvalue (λ_3) measures the degree of contraction parallel to the bond and from the CP toward each of the neighboring nuclei. When the negative eigenvalues dominate, the electronic charge is locally concentrated in the region of the CP leading to an interaction characteristic of covalent or polarized bonds and being characterized by large $\rho(\mathbf{r})$ values, $\nabla^2\rho(\mathbf{r}) < 0$, $|\lambda_1|/\lambda_3 > 1$, and $G/\rho(\mathbf{r}) < 1$, G being the kinetic energy density of the system. If the positive eigenvalue is dominant, on the other hand, the electronic density is locally concentrated at each atomic site. The interaction is now referred to as a closed-shell one, and it is characteristic of highly ionic bonds, hydrogen bonds, and van der Waals interactions. It is characterized by relatively low $\rho(\mathbf{r})$ values, $\nabla^2\rho(\mathbf{r}) > 0$, $|\lambda_1|/\lambda_3 < 1$, and $G/\rho(\mathbf{r}) > 1$. Finally, the ellipticity, ϵ, defined as $\lambda_1/\lambda_2 - 1$, indicates the deviation of the electronic charge density from the axial symmetry, providing a quantitative measure of the π character of the bond.

Results and Discussion

The optimized geometry of the TS calculated for the hydrogen exchange reaction of methane on a zeolite acid site at the B3LYP/6-31G** level of theory is shown in Figure 1. The most relevant geometric parameters of CH_4, CH_5^+, T3, and the TS for that reaction are shown in Table 1. It can be seen that although the TS resembles the interaction between a free carbocation and a negatively charged T3 cluster, the C−H* bond lengths are considerably larger in the TS than in the free CH_5^+. The H*−C−H* bond angle, furthermore, increases its value by about 10° in the TS with respect to the free carbocation. No appreciable changes are observed, on the other hand, for the C−H bonds and H−C−H angles when free methane, free CH_5^+, and TS are compared. The O*−H* bond length in T3 becomes greatly enlarged when the TS is formed. Moreover, a new O**−H* bond evolves, reaching the same value as that of the O*−H* bond in the TS.

The total topology of the TS is consistent with the Poincaré−Hopf relationship, which states that the number of nuclei minus the number of bond CP plus the number of ring CP minus the

TABLE 1: Selected Bond Lenghts (*r*, in Å) and Bond Angles (*a*, in deg) of Optimized Geometries of T3, CH_4, CH_5^+, and TS for the Hydrogen Exchange Reaction of Methane on T3 (1), CH_3^+, and TS for the Dehydrogenation Reaction of Methane on T3 (2) Calculated at the B3LYP/6-31G Level of Theory**

parameter	T3	CH_4	CH_5^+	TS (1)	CH_3^+	TS (2)
r(C−H)		1.092	1.083	1.095	1.094	1.098
r(C−H*)			1.177	1.337		1.680
r(C−O*)						2.646
r(C−O**)						2.162
r(O*−H*)	0.964			1.314[a]		1.694
a(H−C−H)		109.5	108.45	109.9	120.0	118.0
a(H*−C−H*)			47.96	56.2		63.3

[a] O*−H* and O**−H* bond lengths have the same value.

number of box CP must be equal to 1[26] (21 − 21 + 1 + 0 = 1, in the present case).

Table 2 shows the properties of the electronic charge density in some selected bond CP of the studied species. The C−H bonds in methane, free CH_5^+, and the TS have very similar topological properties which are, furthermore, typical of covalent bonds, that is, relatively high values of $\rho(\mathbf{r})$, negative and considerably high values of $\nabla^2\rho(\mathbf{r})$, a value of $|\lambda_1|/\lambda_3$ greater than the unity, and relatively low values of $G/\rho(\mathbf{r})$. The C−H* bonds in the TS, on the other hand, show a rather lower value of $\rho(\mathbf{r})$ and a much less negative value of $\nabla^2\rho(\mathbf{r})$ than in CH_5^+. Moreover, the $|\lambda_1|/\lambda_3$ ratio is slightly less than one in the TS. These values, however, are still within the range of typical covalent interactions. This conclusion is reinforced by the fact that $G/\rho(\mathbf{r})$ is lower than 1 and very similar in both free CH_5^+ and the TS. It is important to note the high ellipticity of the C−H* bond in CH_5^+, thus reflecting a structural instability probably related to the three-center two-electron bond in this species. On the contrary, the ellipticity is considerably lower in the TS, indicating that the above instability is clearly reduced by the interaction of methane with the zeolite. This fact suggests that the zeolite system (represented here by a T3 cluster) is not a simple counterion in the overall process, but it plays an important role leading to a net stabilization of a carbocationlike structure in the TS of the hydrogen exchange reaction of methane on zeolite.

The O*−H* bond in the T3 cluster exhibits the typical characteristics of a covalent bond, that is, relatively high positive values of $\rho(\mathbf{r})$, negative and considerably high values of $\nabla^2\rho(\mathbf{r})$, a $|\lambda_1|/\lambda_3$ ratio greater than 1, and a low value of $G/\rho(\mathbf{r})$. Interestingly, both the O*−H* and O**−H* bonds in TS show a positive curvature of $\rho(\mathbf{r})$, a $G/\rho(\mathbf{r})$ quotient still lower than 1 but much higher than the value found in T3, and a $|\lambda_1|/\lambda_3$ ratio considerably lower than 1, indicating that the electronic density tends to concentrate on the atomic basins. Even though the electronic charge density has a rather small but positive value at the bond CP, these results seem to suggest a rather ionic interaction between a carbocationlike structure and a negatively charged T3 cluster. This finding is clearly in constrast with the results reported by other authors and mentioned in the Introduction.[5−10]

Figures 2−4 show the Laplacian of the electronic charge density for CH_4, CH_5^+, and TS, respectively. The molecular graphs are also indicated.

As can be seen in Figure 2, the C−H bonds in methane are clearly covalent, showing a considerable concentration of electronic charge in the internuclear region.

The relatively small H*−C−H* bond angle in CH_5^+ yields to an electronic charge density concentration involving the three atoms giving place to a three-center two-electron bond well characterized by the topology of $\nabla^2\rho(\mathbf{r})$ (see Figure 3).

Figure 4 clearly shows that as a consequence of the H*−C−H* angle opening in the TS, the electronic charge density is much less concentrated between the three atoms, as it should be expected. This fact seems to reinforce the argument that no free carbocation is present in the TS for the process under study. On the other hand, it is also evident from Figure 4 that both O*−H* and O**−H* bonds in TS correspond to closed-shell interactions. This is in contrast to what is found in the T3 cluster for the O*−H* bond, that is, a clear covalent interaction.

It is also interesting to stress the very different roles played by the O* and O** atoms in the TS formation. The O* atom acts as a Brønsted acid releasing a hydrogen atom which tends to bond the C atom in methane. The O** atom, on the other hand, plays the role of a Lewis base stabilizing one of the H atoms of methane through a closed-shell interaction.

Figure 5 shows the calculated TS for the reaction of dehydrogenation of methane on a zeolite acid site. Table 1 provides the most relevant geometric parameters of CH_4, CH_3^+, the T3 cluster, and TS for the reaction under study. It can be seen in the figure that the carbon-containing fragment in TS presents C−H bond distances very similar to that found in free CH_3^+ and a H−C−H bond angle very close to that corresponding to the planar geometry. The H* atom originally belonging to the methane molecule is located in the TS very far from the fragment to be considered still bonded to the carbon atom. The same behavior is observed in the zeolitic fragment in which the O*−H* bond distance increases its value from 0.96 Å to almost 1.70 Å. Moreover, the H*−H* bond distance is slightly larger than the equilibrium H−H bond length of 0.74 Å, calculated at the B3LYP/6-31G** level of theory. It can also be seen in the figure that the carbon atom is bonded to the O* and O** atoms of the T3 cluster in a nonsymmetric way, being closer to the oxygen atom that bears no hydrogen atom in the isolated T3 cluster. The TS for the process under study would be then characterized as formed by three weakly interacting fragments, namely, a CH_3^+ carbocation, a H_2 promolecule, and a negatively charged T3 cluster.

Once again, the total topology of the TS is consistent with the Poincaré−Hopf relationship.

Table 3 shows the properties of the electronic charge density in some selected bond CP of CH_4, CH_3^+, T3, and the TS. Reinforcing the arguments derived from the geometric parameters, it can be seen that C−H bonds in methane, the carbenium ion, and the TS present very similar topological properties, all of these being characteristic of covalent bonds. The C−H* bond in the TS, on the contrary, has a very low, although still greater than zero, value of $\rho(\mathbf{r})$, a positive value of $\nabla^2\rho(\mathbf{r})$, and a $|\lambda_1|/\lambda_3$ ratio lower than the unity. Furthermore, the $G/\rho(\mathbf{r})$ ratio considerably enhances its value with respect to the C−H bonds. These facts suggests that the C−H* bond can be described as a closed-shell type interaction.

The carbon atom of methane interacts with the two bridge oxygen atoms of the T3 cluster when the TS is formed. Both the C−O* and C−O** bonds present rather low and positive values of $\rho(\mathbf{r})$, $|\lambda_1|/\lambda_3$ ratios noticeably lower than 1, and positive values of $\nabla^2\rho(\mathbf{r})$, magnitudes higher in the last case. Furthermore, these bonds also show a $G/\rho(\mathbf{r})$ ratio very close to unity. These features allow us to consider the C−O interactions as weak, closed-shell ones. It should be also noted that both bonds exhibit noticeably high values of ϵ, a fact that can be interpreted as a trend to undergo structural changes.

TABLE 2: Topological Properties (in au) of the Electronic Charge Density in Selected Bond CP of CH_4, CH_5^+, T3, and TS for the Hydrogen Exchange Reaction of Methane on T3[a]

system	bond	$\rho(\mathbf{r})$	$\nabla^2\rho(\mathbf{r})$	λ_1	λ_2	λ_3	$\lvert\lambda_1\rvert/\lambda_3$	ϵ	$G/\rho(\mathbf{r})$
CH_4	C−H	0.2716	−0.8959	−0.6931	−0.6931	0.4903	1.4136	0.0000	0.1594
CH_5^+	C−H	0.2894	−1.1000	−0.8217	−0.7973	0.5190	1.5832	0.0305	0.0950
	C−H*	0.2249	−0.5458	−0.4987	−0.1637	0.1166	4.2770	2.0471	0.2686
T3	O*−H*[b]	0.3540	−2.4864	−1.7823	−1.7572	1.0532	1.6923	0.0143	0.1839
TS	C−H	0.2667	−0.8551	−0.6823	−0.6635	0.4907	1.3905	0.0283	0.1706
	C−H*	0.1504	−0.2377	−0.3457	−0.2764	0.3844	0.8993	0.2508	0.2633
	O*−H*[c]	0.1287	0.0225	−0.3439	−0.3389	0.7052	0.4877	0.0148	0.6193

[a] See Method and Calculation details for an explanation of the symbols. [b] This is the only O−H bond in the isolated T3. [c] The O*−H* and O**−H* bonds share the same topological properties.

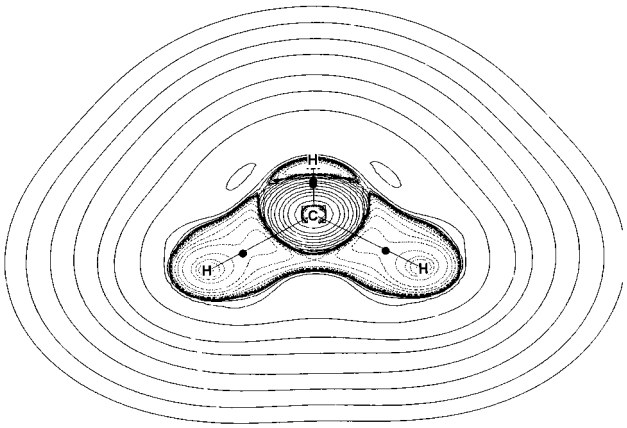

Figure 2. Laplacian of the electronic charge density of CH_4. The plane containing a H−C−H group is shown. Solid lines represent regions of electronic charge concentration and, broken lines denote regions of electronic charge depletion. Bond CP and ring CP are indicated with circles and triangles, respectively. The molecular graph is also indicated. The contours of the Laplacian of the electronic charge density increase and decrease from a zero contour in steps of $\pm 2 \times 10^n$, $\pm 4 \times 10^n$, and $\pm 8 \times 10^n$, with n beginning at -3 and increasing by unity. The same set of contours is used in all the figures of the present work.

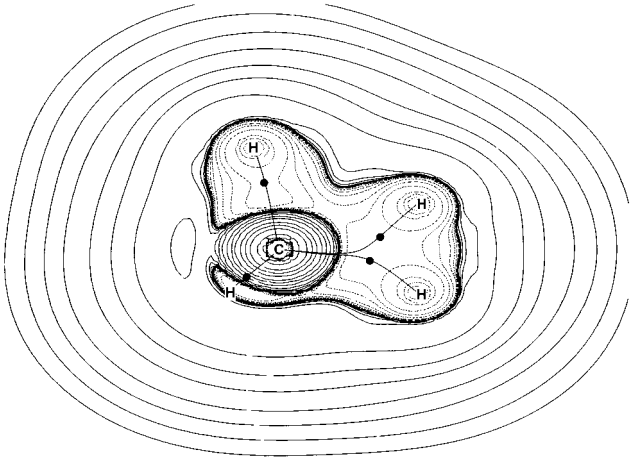

Figure 3. Laplacian of the electronic charge density of CH_5^+. The plane containing the H*−C−H* group is shown. Solid lines represent regions of electronic charge concentration, and broken lines denote regions of electronic charge depletion. Bond CP and ring CP are indicated with circles and triangles, respectively. The molecular graph is also indicated.

The O*−H* bond shows the characteristic properties of covalent interactions in the T3 cluster, namely, an appreciable and positive value of $\rho(\mathbf{r})$, a large and negative value of $\nabla^2\rho(\mathbf{r})$, a $G/\rho(\mathbf{r})$ ratio much less than 1, and a $|\lambda_1|/\lambda_3$ ratio considerably higher than the unity. The O*−H* bond in the TS, on the other hand, presents noticeable changes in those properties, indicating

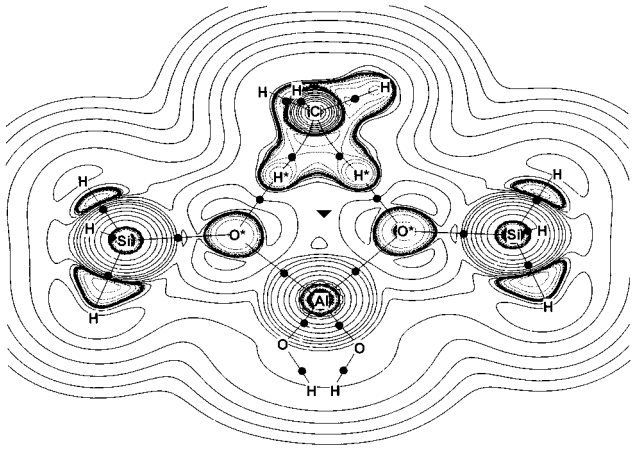

Figure 4. Laplacian of the electronic charge density of the TS for the hydrogen exchange reaction of methane on a T3 cluster. The plane containing C, H*, O*, and O** atoms is shown. Solid lines represent regions of electronic charge concentration, and broken lines denote regions of electronic charge depletion. Bond CP and ring CP are indicated with circles and triangles, respectively. The molecular graph is also indicated.

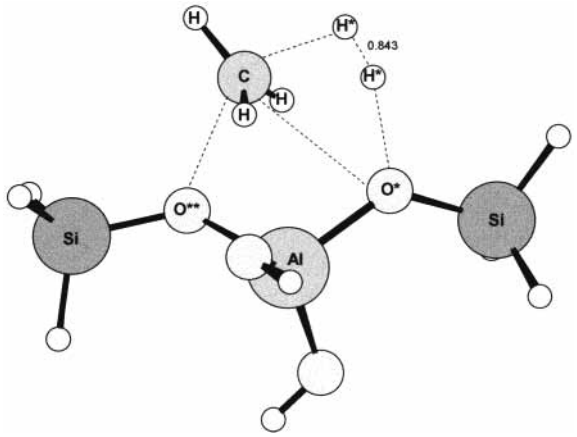

Figure 5. Transition state geometry for the dehydrogenation reaction of methane on a T3 cluster. See Tables 1 and 2 for labels.

that the electronic charge density is preferably concentrated on the atomic basins.

Finally, the H*−H* bond can be characterized as a covalent interaction according to the topological properties shown in Table 3. Furthermore, these magnitudes are not very different from the corresponding values for H_2 evaluated at the B3LYP/6-31G** level of theory, too.

Figures 6 and 7 show the Laplacian of the electronic charge density for CH_3^+ and the TS, respectively.

As can be seen in Figure 6, the C−H bonds in CH_3^+ ion are clearly covalent, with a considerable concentration of electronic charge density in the internuclear region.

TABLE 3: Topological Properties (in au) of the Electronic Charge Density in Selected Bond CP of CH_4, CH_3^+, T3, and TS for the Dehydrogenation Reaction of Methane on T3

system	bond	$\rho(\mathbf{r})$	$\nabla^2\rho(\mathbf{r})$	λ_1	λ_2	λ_3	$\lvert\lambda_1\rvert/\lambda_3$	ϵ	$G/\rho(\mathbf{r})$
CH_4	C−H	0.2716	−0.8959	−0.6931	−0.6931	0.4903	1.4136	0.0000	0.1594
CH_3^+	C−H	0.2909	−1.1277	−0.9089	−0.8600	0.6412	1.4175	0.0568	0.0546
T3	O*-H*	0.3540	−2.4864	−1.7823	−1.7572	1.0532	1.6923	0.0143	0.1839
TS	C−H	0.2909	−1.0587	−0.8476	−0.8204	0.6093	1.3911	0.0332	0.0918
	C−H*	0.0667	0.0856	−0.0778	−0.0723	0.2357	0.3301	0.0761	0.5397
	C−O**	0.0477	0.1515	−0.0527	−0.0314	0.2357	0.2236	0.6782	0.8155
	C−O*	0.0219	0.0968	−0.0147	−0.0088	0.1204	0.1221	0.6699	0.9680
	H*−H*[b]	0.1999	−0.6838	−0.6028	−0.5868	0.5059	1.1915	0.0272	0.0505
	O*−H*	0.0513	0.1178	−0.0850	−0.0824	0.2853	0.2979	0.0323	0.7134

[a] See Method and Calculation details for an explanation of the symbols. [b] ρ and $\nabla^2\rho$ equal 0.2618 and −1.0614 au, respectively, for isolated H_2 calculated at the B3LYP/6-31G** level of theory.

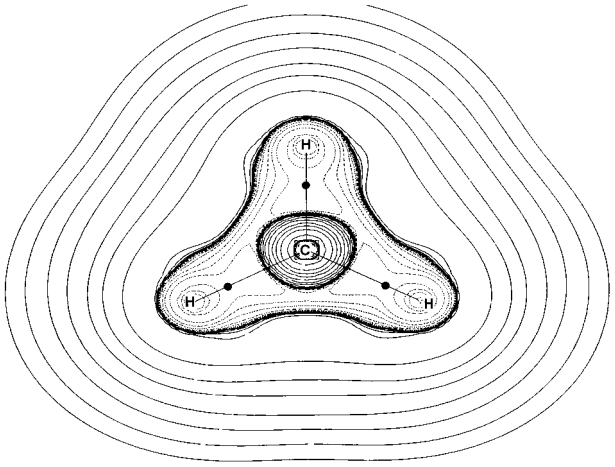

Figure 6. Laplacian of the electronic charge density of CH_3^+. The molecular plane is shown. Solid lines represent regions of electronic charge concentration, and broken lines denote regions of electronic charge depletion. Bond CP and ring CP are indicated with circles and triangles, respectively. The molecular graph is also indicated.

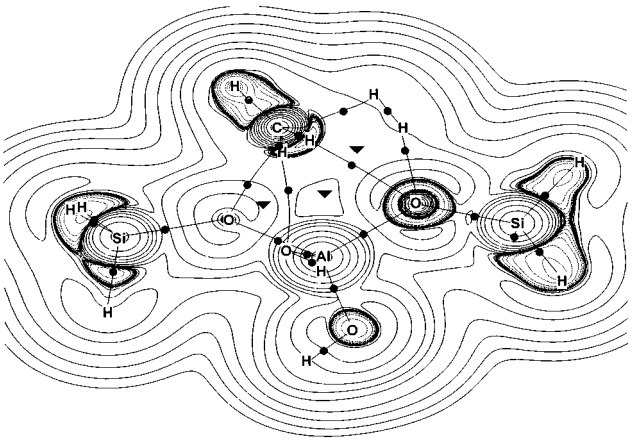

Figure 7. Laplacian of the electronic charge density of the TS for the dehydrogenation reaction of methane on a T3 cluster. The plane containing the C, O*, O**, and H* atoms is shown. Solid lines represent regions of electronic charge concentration, and broken lines denote regions of electronic charge depletion. Bond CP and ring CP are indicated with circles and triangles, respectively. The molecular graph is also indicated.

Several interesting features can be appreciated in Figure 7. An electronic charge density concentration evolves along both the C−H and H*−H* bonds. Moreover, the carbon-containing fragment shows an electronic charge density distribution very similar to that observed in free CH_3^+ (see Figure 6). On the other hand, it is clear in the figure that the bond CP corresponding to the C−O**, C−H*, and O*−H* interactions are located in regions charaterized by an electronic charge density depletion. These findings suggest that the TS for the dehydrogenation reaction of methane on a zeolite can be well described as a weak interaction with dominant ionic character.

In the present process, the dehydrogenation reaction of methane on a zeolitic system, the O* atom acts again as a Brønsted acid releasing a hydrogen atom which begins to form dihydrogen. On the other hand, the O** atom contributes to the stabilization of the carbon-containing fragment through a weak, closed-shell type electrostatic interaction.

Conclusions

A topological study of the transition states arising in the hydrogen exchange and deydrogenation reactions of methane on a zeolite acid site represented by a T3 cluster is accomplished in this work within the framework of the density functional theory.

It is found that no free methonium cation, CH_5^+, is presented in the transition state for the hydrogen exchange reaction. A similar structure with larger C−H bond lengths and H−C−H angle evolves instead being further stabilized by two zeolitic oxygen atoms. The interaction between the carbocationlike structure and the negatively charged T3 cluster can be described as a rather ionic interaction instead of a purely covalent one, in which the zeolite plays an important role diminishing some structural instabilities found in the free CH_5^+ ion.

The transition state in the dehydrogenation reaction of methane on a zeolite acid site can be properly characterized as a weak, closed-shell interaction between three different fragments, namely, a CH_3^+ carbocation, a H_2 pseudomolecule, and a negatively charged T3 cluster. The cationic fragment shows geometric parameters and topological properties very similar to those found in free CH_3^+. Although it exhibits a bond length larger than the equilibrium H−H bond distance, the H_2 fragment is clearly characterized by a covalent interaction.

The oxygen atom bearing the hydrogen atom in the isolated T3 cluster acts as a Brønsted acid in the two processes under study. The other oxygen atom belonging to the T3 cluster, on the contrary, plays the role of a Lewis base stabilizing a hydrogen atom of the incoming methane molecule in the hydrogen exchange reaction and directly interacting with the carbon atom of methane in the dehydrogenation process.

Acknowledgment. The authors acknowledge the Supercomputer Center of the Secretary for the Technology, Science, and Productive Innovation, Argentine, for computational time. N.B.O. thanks SECYT-UNNE for a scholarship. R.P.D. and A.H.J. are members of the Scientific Research Careers of CONICET and CICPBA, Argentine, respectively. C.J.A.M.

thanks PRONEX, CNPq, and FAPERJ for financial support. P.M.E. thanks FAPERJ for a fellowship.

References and Notes

(1) Corma, A. *Chem. Rev.* **1995**, *95*, 559.
(2) Boronat, M.; Viruela, P.; Corma, A. *J. Phys. Chem. A* **1998**, *102*, 9863.
(3) Blaszkowski, S. R.; van Santen, R. A. *Top. Catal.* **1997**, *4*, 145.
(4) Rigby, A. M.; Kramer, G. L.; van Santen, R. A. *J. Catal.* **1997**, *170*, 1.
(5) Kramer, G. J.; van Santen, R. A.; Emeis, C. A.; Novak, A. K. *Nature* **1993**, *363*, 529.
(6) Blaszkowski, S. R.; Jansen, A. P. J.; Nascimento, M. A. C.; van Santen, R. A. *J. Phys. Chem.* **1994**, *98*, 12938.
(7) Kramer, G. J.; van Santen, R. A. *J. Am. Chem. Soc.* **1995**, *117*, 1766.
(8) Kramer, G. J.; van Santen, R. A. *Chem. Rev.* **1995**, *95*, 637.
(9) van Santen, R. A. *Catal. Today* **1997**, *38*, 377.
(10) Esteves, P. M.; Nascimento, M. A. C.; Mota, C. J. A. *J. Phys. Chem. B* **1999**, *103*, 10417.
(11) Wang, L.; Tao, L.; Xie, M.; Xu, G.; Huang, J.; Xu, Y. *Catal. Lett.* **1993**, *21*, 35.
(12) Lins, J. O. M. A.; Nascimento, M. A. C. *J. Mol. Struct. (THEOCHEM)* **1996**, *371*, 237.
(13) Kazansky, V. B.; Frash, M. V.; van Santen, R. A. *Catal. Lett.* **1994**, *28*, 211.
(14) Blaszkowski, S. R.; Jansen, A. P. J.; Nascimento, M. A. C.; van Santen, R. A. *J. Phys. Chem.* **1994**, *98*, 11332.
(15) Evleth, E. M.; Kassab, E.; Sierra, L. R. *J. Phys. Chem.* **1994**, *98*, 1421.
(16) (a) Hohenberg, P.; Kohn, W. *Phys. Rev. B* **1964**, *136*, 864. (b) Kohn, W.; Sham, L. J. *Phys. Rev. A* **1965**, *140*, 1133. (c) Parr, R. G.; Yang, W. *Density Functional Theory of Atoms and Molecules*; Oxford University Press: Oxford, 1989.
(17) Bader, R. F. W. *Atoms in Molecules. A Quantum Theory*; Clarendon: Oxford, 1990.
(18) Popelier, P. L. A. *Atoms in Molecules. An Introduction*; Pearson Education: Harlow, U.K., 1999.
(19) Becke, A. D. *J. Chem. Phys.* **1993**, *98*, 5648.
(20) Lee, C.; Yang, W.; Parr, R. G. *Phys. Rev. B* **1988**, *37*, 785.
(21) Frisch, M. J.; Trucks, G. W.; Schlegel, H. B.; Gill, P. M. W.; Johnson, B. G.; Robb, M. A.;. Cheeseman, J. R; Keith, T.; Petersson, G. A.; Montgomery, J. A.; Raghavachari, K.; Al-Laham, M. A.; Zakrzewski, V. G.; Ortiz, J. V.; Foresman, J. B.; Cioslowski, J.; Stefanov, B. B.; Nanayakkara, A.; Challacombe, M.; Peng, C. Y.; Ayala, P. Y.; Chen, W.; Wong, M. W.; Andres, J. L.; Replogle, E. S.; Gomperts, R.; Martin, R. L.; Fox, D. J.; Binkley, J. S.; Defrees, D. J.; Baker, J.; Stewart, J. P.; Head-Gordon, M.; Gonzalez, C.; Pople, J. A. *Gaussian 94*, Revision E.1; Gaussian, Inc.: Pittsburgh, PA, 1995.
(22) (a) Baker, J. *J. Comput. Chem.* **1986**, *7*, 385. (b) Baker, J. *J. Comput. Chem.* **1987**, *8*, 563.
(23) Blieger-Konig, F. W.; Bader, R. F. W.; Tang, T. H. *J. Comput. Chem.* **1982**, *3*, 317.
(24) Bader, R. F. W. *J. Phys. Chem. A* **1998**, *102*, 7314.
(25) Cremer, D.; Kraka, E.; Slee, T. S.; Bader, R. F. W.; Lau, C. D. H.; Nguyen-Dang, T. T.; MacDougall, P. J. *J. Am. Chem. Soc.* **1983**, *105*, 5069.
(26) Collard, K.; Hall, G. G. *Int. J. Quantum Chem.* **1977**, *12*, 623.